A Discrete-Time Filter for the Generation of Signals with Asymmetric and Variable Bounds on Velocity, Acceleration, and Jerk

Corrado Guarino Lo Bianco, *Member, IEEE,* and Fabio Ghilardelli

***Abstract*—Reference signals, that are used to drive feedback control loops, are often evaluated on-the-fly on the basis of the operating conditions. As a consequence, they can be too demanding for the actuation system which outputs could saturate, thus worsening the tracking performances of the feedback loop. Improved answers can be obtained by smoothing rough references by means of proper filters that are also able to impose bounds on the signal dynamics. The paper proposes a filtering system which output mimics at best any given input signal compatibly with some smoothness requirements. In particular, generated signals are continuous up to the second time derivative and their first three time derivatives are constrained between assigned bounds that can be asymmetric and that can also be changed on-the-fly. The filter, that is internally characterized by minimum time transients, is able to follow, with zero tracking error, piecewise-continuous signals given by combinations of steps, ramps, and parabolas.**

***Index Terms*—Dicrete time filters, jerk constraints, minimum time, signal generators, variable structure systems.**

I. Introduction

The smoothness of the reference signals has a strong impact on the behavior of the control systems. It is well known, indeed, that system performances generally improve when smooth signals are used. For this reason, reference signals that admit bounded first, second and third time derivatives are commonly adopted in industrial applications.

Preliminary works addressed the reference generation problem by means of offline strategies. For example, minimum-time trajectories, that satisfy the above mentioned constraints, were planned in [1], by means of a polyhedron search strategy. A similar problem was studied in [2], by also considering constraints on the actuator torques. The solution was found by adopting a sensitivity approach.

Offline strategies return solutions that are tailored for particular configurations and applications. Conversely, in industrial contexts, rapidly mutating scenarios, that require continuously changing strategies, must be often considered. The online generation of minimum time trajectories, subject to constraints on velocities, accelerations, and jerks, was first addressed in [3]. The problem was solved by means of a direct planning strategy based on the use of a near time-optimal solver. An alternative online method, based on the discretization of the minimum-time problem, has been proposed in [4]. In the same paper, a comparison with two sequential quadratic programming approaches is carried out. It shows that, with direct planning methods and with the current technology, optimal trajectories can be generated in milliseconds. If shorter evaluation times are required because of the sampling time of the governed system, alternative solutions must be investigated. Most of them consider rest-to-rest transients and static constraints. This is the case, for example, of the closed form solution that was proposed in [5]–[7], in which asymmetric S-curves were adopted in order to reduce the vibrations that occur during arrest transients. Time optimality was not specifically addressed. A totally different approach was considered in [8], where constrained minimum-time trajectories were generated by means of FIR filters. The Neuro-Fuzzy approach in [9] overcomes some of the limitations that characterize previous methods: The trajectory can start from generic initial conditions and the constraints are not static.

The study has been enlarged in [10], [11] by considering multidimensional motions. Minimum-time online trajectories were generated for step reference signals by considering constraints on velocities, accelerations and jerks. In [12] still considering the same constraints, variable reference signals were accounted for. The approaches proposed in [10]–[12] have a common characteristic: The problem is deeply investigated offline, so that online evaluations are performed in microseconds. The sole drawback of these approaches is represented by the complexity of the planning algorithm, that can be reduced, still with computational times of microseconds, by adopting indirect planning methods, i.e., by generating trajectories through proper feedback systems. Early works on this topic appeared in [13]–[15] and in [16], [17] respectively for continuous and discrete-time frameworks. Given solutions were based on second order filters that were able to impose bounds on the velocity and on the acceleration signals. Such kind of planning strategies have been widely employed in actual real-time applications [18]–[23] because, if compared with previously cited direct planning methods, they are characterized by several advantages: Trajectories are not limited to rest-to-rest movements but, conversely, generic initial and final conditions can be handled, constraints can be changed in real-time, and, finally, the code that is required for their implementation is extremely compact and efficient, so that it can be executed with industrial microcontroller boards.

Manuscript received May 22, 2013; Accepted for publication Sept. 4, 2013.

This work was partially supported by MIUR in the framework of a PRIN2010-11 project (MARIS - Marine Autonomous Interventions).

The Authors are with the Dip. di Ing. dell'Informazione, University of Parma, Italy; e-mail: {guarino,fghilardelli}@ce.unipr.it.

In a continuous-time context, the first proposal of a jerk-limited feedback planner was made in [24] with a scheme that was able to generate trajectories characterized by bounded velocities, accelerations and jerks. The planner did not handle generic interpolating conditions but, conversely, it was only able to drive the system toward the rest status.

The first third-order continuous-time solution, that was able to manage generic interpolating conditions, was proposed in [25]. Its discrete-time implementation was affected by jerk chattering and transient overshoots (see [26]). The dicrete-time scheme, that was later proposed in [27] in order to deal with these problems, was only able to account for the jerk bounds. Such solution has been improved in [28] with a strategy that simultaneously handles velocity, acceleration and jerk limits: The jerk chattering problem was eliminated but, for particular interpolating conditions, the overshoot issue, caused by suboptimal transients, is still present.

The nonlinear variable-structure filter proposed in this paper solves the following challenging problem: Given a piecewise continuous input signal, it generates a smooth output reference that represents its best possible approximation compatibly with some assigned bounds on velocities, accelerations and jerks. The admissible bounds can be asymmetric and can be changed online. The bounds asymmetry is a novelty with respect to any other solution proposed in the literature and it is essential in order to handle applications like those described, e.g., in [29]. Furthermore, the new filter always guarantees minimum-time transients and eliminates the overshoot problem that was affecting the analogous filter proposed in [28].

The characteristics of the new filter can be summarized as follows: Generic initial and final conditions can be assumed on position, velocity, and acceleration; the output signal is continuous up to the second time derivative; the output trajectory fulfills any given asymmetric constraint on velocity, acceleration and jerk; constraints can be freely changed, also during transients; transients are always minimum-time; the reference input signal is reached without overshoot compatibly with the given constraints; the jerk signal is not affected by the chattering phenomenon. The filter is stabilized by means of an Algebraic Variable Structure Controller (AVSC) based on sliding mode techniques. As known, such kind of control techniques are very often used in industrial contexts [30]–[33] because of their robustness and because of the compactness of the code that is required for their implementation.

The paper is organized as follows. In §II the problem is formulated and the novel third-order discrete-time filter is proposed. Convergence properties of the filter are analyzed in §III, in §IV, and in §V. The performances of the new filter are compared in §VI with those of the filter proposed in [28]. In the same section a new test case is discussed, while §VII reports some final conclusions.

II. The optimal trajectory scaling problem and the discrete-time filter

Let us consider the following definition

Definition 1: A function

$$\begin{array}{rcl} f : [0, t_f] & \rightarrow & \mathbb{R} \\ t & \rightarrow & f_d := f(t) \end{array}$$

is *feasible*, and we write $f \in \mathcal{F}$, if it is continuous together with its first and second time derivatives and if it fulfills the following constraints

$$\begin{array}{ll} R^- \leq \dot{f}(t) \leq R^+, & \forall t \in [0, t_f], \\ S^- \leq \ddot{f}(t) \leq S^+, & \forall t \in [0, t_f], \\ U^- \leq \dddot{f}(t) \leq U^+, & \forall t \in [0, t_f]. \end{array}$$

where $R^-, S^-, U^- \in \mathbb{R}^-$ and $R^+, S^+, U^+ \in \mathbb{R}^+$ are freely assignable bounds.

The nonlinear discrete-time filter proposed in this paper solves the following problem:

Problem 1: Given a piecewise reference signal $r(t)$ made of steps, ramps or parabolas, evaluate an optimal output signal $x(t)$, which is continuous together with its first and second time derivatives, by solving one of the following optimality problems, selected on the basis of the feasibility of $x(0)$ and $r(t)$:

a) $x(0) \notin \mathcal{F}$
$\min_{x(t)} t_f$ subject to $x(t_f) \in \mathcal{F}$.
t_f evidently indicates the instant in which $x(t)$ becomes feasible.

b) $r(t) \notin \mathcal{F}$ and $x(0) \in \mathcal{F}$
$\min_{x(t)} \int |r(\tau) - x(\tau)|\, d\tau$ subject to $x(t) \in \mathcal{F}$.

c) $r(t) \in \mathcal{F}$ and $x(0) \in \mathcal{F}$
$\min_{x(t)} t_f$ subject to $r(t_f) - x(t_f) = 0$ and to $x(t) \in \mathcal{F}, \quad \forall t \in [0, t_f]$.
t_f is evidently the instant in which $x(t)$ hangs $r(t)$. The tracking condition must be obtained, compatibly with the given bounds, without overshoot.

Roughly speaking, if $x(0) \notin \mathcal{F}$, then feasibility must be gained in minimum time, otherwise two different situations could occur: If $r(t) \notin \mathcal{F}$, then $x(t)$ must be its best feasible approximation, while, $r(t)$ must be hanged in minimum time if $r(t) \in \mathcal{F}$. Evidently, feasibility represents the prior target of the system. The bounds could be time-varying and can also be changed during transients. Analogously, $r(t)$ could be modified at any time, so that the solution of Problem 1 must be evaluated at each sample time. Since control systems are mainly governed by means of digital controllers, a discrete time solution of Problem 1 is proposed. In the following, subscript $i \in \mathbb{N}$ indicates sampled variables that are acquired at time $t = iT$, where T is the system sampling time.

The problem is clearly similar to the one that was considered in [28], but, as a novelty, asymmetric jerk constraints are handled. Moreover, in [28], under particular operating conditions, some transients toward r were suboptimal and characterized by overshoot issues: The new solution totally eliminates both problems. These improvements, that are essential to manage problems like the one, e.g., that was proposed in [29], have required a complete redefinition of the filter control laws. Practically, while the structure of the discrete-time filter, that is shown in Fig. 1, is the same that was proposed in [28], i.e., it is made of a chain of three integrators, the AVSC has been completely rewritten in order to fulfill the new requirements. The AVSC is based on sliding mode techniques [34], and

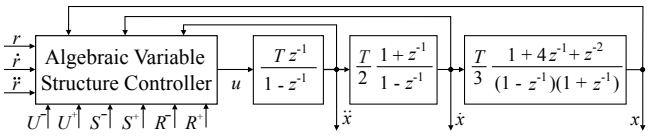

Fig. 1. The discrete-time system that solves *Problem* 1. The system is composed by a dynamic chain based on three integrators and an algebraic variable-structure controller.

uses a combination of appropriate Sliding Surfaces (SS) to robustly stabilize the system and to solve *Problem* 1. The system dynamics is only due to the integrators chain and can be represented as follows

$$\mathbf{x}_{i+1} = \mathbf{A}\,\mathbf{x}_i + \mathbf{b}\,u_i\ , \tag{1}$$

where $\mathbf{x}_i := [x_i\ \dot{x}_i\ \ddot{x}_i]^T$ is the system state and

$$\mathbf{A} = \begin{bmatrix} 1 & T & \frac{T^2}{2} \\ 0 & 1 & T \\ 0 & 0 & 1 \end{bmatrix}\ , \quad \mathbf{b} = \begin{bmatrix} \frac{T^3}{6} \\ \frac{T^2}{2} \\ T \end{bmatrix}\ . \tag{2}$$

Reference signal r_i is evaluated as follows

$$\mathbf{r}_{i+1} := \mathbf{A}\,\mathbf{r}_i\ , \tag{3}$$

where $\mathbf{r}_i := [r_i\ \dot{r}_i\ \ddot{r}_i]^T$. A step, a ramp, or a parabola can be generated depending on the initial values that are chosen for $\dot{r}_i$ and $\ddot{r}_i$. According to the hypothesis, $\dddot{r}_i = 0$.

In order to formulate the control law for the AVSC, let us first consider the following change of coordinates $y_i := x_i - r_i$, $\dot{y}_i := \dot{x}_i - \dot{r}_i$, $\ddot{y}_i := \ddot{x}_i - \ddot{r}_i$, that places the system origin on the trajectory to be tracked. Due to (3), system (1) becomes

$$\mathbf{y}_{i+1} = \mathbf{A}\,\mathbf{y}_i + \mathbf{b}\,u_i\ , \tag{4}$$

where $\mathbf{A}$ and $\mathbf{b}$ coincide with (2), while $\mathbf{y}_i := [y_i\ \dot{y}_i\ \ddot{y}_i]^T$.

A further change of coordinates $\mathbf{y}_i = \mathbf{W}\,\mathbf{z}_i$, where

$$\mathbf{W} := \begin{bmatrix} T^3 & -T^3 & \frac{T^3}{6} \\ 0 & T^2 & -\frac{T^2}{2} \\ 0 & 0 & T \end{bmatrix}\ , \tag{5}$$

is required to eliminate sampling time T from matrices $\mathbf{A}$ and $\mathbf{b}$. System (4) becomes

$$\mathbf{z}_{i+1} = \mathbf{A}_d\,\mathbf{z}_i + \mathbf{b}_d\,u_i\ , \tag{6}$$

where $\mathbf{z}_i := [z_{1,i}\ z_{2,i}\ z_{3,i}]^T$ and

$$\mathbf{A}_d = \begin{bmatrix} 1 & 1 & 1 \\ 0 & 1 & 1 \\ 0 & 0 & 1 \end{bmatrix}\ , \quad \mathbf{b}_d = \begin{bmatrix} 1 \\ 1 \\ 1 \end{bmatrix}\ . \tag{7}$$

Matrix $\mathbf{W}$ is non singular, so that inverse transformation $\mathbf{z}_i = \mathbf{W}^{-1}\,\mathbf{y}_i$ exists with certainty.

The proposed controller is designed to force state $\mathbf{z}$ toward the origin in minimum time by means of transients which fulfill the given constraints on velocity, acceleration, and jerk. If this result is achieved, then, $\mathbf{y} = \mathbf{W}\,\mathbf{z} = \mathbf{0}$ and, in turn, x, as desired, hangs reference r.

The AVSC, that is used to control system (6), depends on system state $\mathbf{z}$ and on the input reference signal, i.e., on $r, \dot{r}, \ddot{r}$. In particular, the following sliding mode control law has been

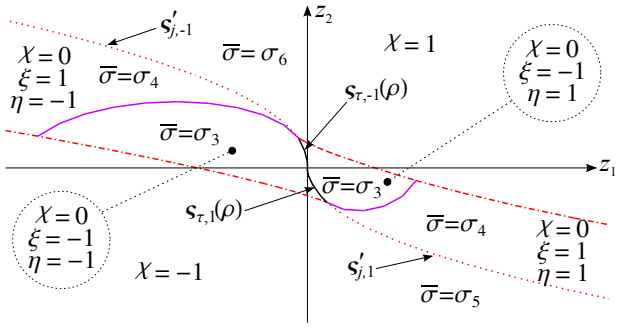

Fig. 2. Partitions of the (z_1, z_2)-plane that are used to select the most appropriate sliding surface. Curve $\varsigma'_{j,1}$ is given by the intersection between σ_4 and σ_5, while $\varsigma'_{j,-1}$ is given by the intersection between σ_4 and σ_6. Curve $\varsigma_{\tau,\eta}$ represent the borderlines between the areas where $\eta = 1$ and $\eta = -1$.

explicitly designed to solve *Problem* 1 (sampling time i has been omitted in the following for conciseness, so that, e.g., command signal u_i is simply indicated as u)

$$u := \begin{cases} -U^- \mathrm{sat}\left(\dfrac{z_3 - \sigma}{U^-}\right) & \text{if} \quad z_3 - \sigma \geq 0 \\ -U^+ \mathrm{sat}\left(\dfrac{z_3 - \sigma}{U^+}\right) & \text{if} \quad z_3 - \sigma < 0 \end{cases}\ , \tag{8}$$

where σ is a SS that depends on z_1 and z_2, while $\mathrm{sat}(\cdot)$ represents a function that saturates its argument to ± 1. Evidently, due to (8), the jerk constraint is certainly satisfied since $u \in [U^-, U^+]$. Equation (8) also defines a Boundary Layer (BL) around the SS. Its upper bound is equal to $\sigma - U^-$, while its lower bound is equal to $\sigma - U^+$.

The SS has a variable structure that depends on $\mathbf{z}$. It is obtained by switching among several SSs according to the following rule

$$\sigma := \begin{cases} \sigma_1 & \text{if} \quad \sigma_1 < \overline{\sigma} \\ \overline{\sigma} & \text{if} \quad \sigma_2 \leq \overline{\sigma} \leq \sigma_1 \\ \sigma_2 & \text{if} \quad \overline{\sigma} < \sigma_2 \end{cases}\ . \tag{9}$$

The equations of σ_1 and σ_2 will soon be given, while $\overline{\sigma}$ is composed itself by several SSs. More precisely, the (z_1, z_2)-space, i.e., the space in which the first two components of the state span, is partitioned into the macro-areas that are shown in Fig. 2 and each of them is unambiguously identified by means of three parameters $\chi = -1, 0, 1$, $\eta = \pm 1$, and $\xi = \pm 1$. Depending on the state location, the most appropriate SS is chosen according to the following rules

$$\overline{\sigma} := \begin{cases} \sigma_3 & \text{if} \quad \chi = 0\ \&\ \xi = -1 \\ \sigma_4 & \text{if} \quad \chi = 0\ \&\ \xi = 1 \\ \sigma_5 & \text{if} \quad \chi = 1 \\ \sigma_6 & \text{if} \quad \chi = -1 \end{cases}\ . \tag{10}$$

Surface $\overline{\sigma}$, that is obtained by composing σ_3, σ_4, σ_5, and σ_6, is continuous and covers the whole (z_1, z_2)-space. All SSs are defined in the following:

1) Surfaces σ_1 and σ_2 (in the following $n = 1, 2$)

$$\sigma_n := -\frac{\gamma_n}{m_n} - \frac{m_n - 1}{2}\kappa_n + \overline{z}_3^+\ , \tag{11}$$

where γ_n, κ_n, and m_n are evaluated as follows

$$z_3^- := \tfrac{S^- - \ddot{r}}{T}, \quad z_3^+ := \tfrac{S^+ - \ddot{r}}{T}, \tag{12}$$

$$\overline{\mathbf{z}}^+ := [\overline{z}_2^+ \ \overline{z}_3^+]^T := \left[\left(\tfrac{R^+ - \dot{r}}{T^2} - \tfrac{\ddot{r}}{2T}\right) \ -\tfrac{\ddot{r}}{T}\right]^T, \tag{13}$$

$$\overline{\mathbf{z}}^- := [\overline{z}_2^- \ \overline{z}_3^-]^T := \left[\left(\tfrac{R^- - \dot{r}}{T^2} - \tfrac{\ddot{r}}{2T}\right) \ -\tfrac{\ddot{r}}{T}\right]^T, \tag{14}$$

$$\hat{z}_3^+ := z_3^+ - \overline{z}_3^+ , \quad \hat{z}_3^- := z_3^- - \overline{z}_3^- ,$$

$$\hat{z}_2^+ := -\left\lceil -\tfrac{\hat{z}_3^+}{U^-} \right\rceil \left[\hat{z}_3^+ + \tfrac{U^-}{2}\left(\left\lceil -\tfrac{\hat{z}_3^+}{U^-} \right\rceil - 1\right)\right] ,$$

$$\hat{z}_2^- := -\left\lceil -\tfrac{\hat{z}_3^-}{U^+} \right\rceil \left[\hat{z}_3^- + \tfrac{U^+}{2}\left(\left\lceil -\tfrac{\hat{z}_3^-}{U^+} \right\rceil - 1\right)\right] ,$$

$$d_1 := z_2 - \overline{z}_2^+ , \quad d_2 := z_2 - \overline{z}_2^- ,$$

$$\gamma_n := \begin{cases} \hat{z}_2^+ & \text{if } d_n < \hat{z}_2^+ \\ d_n & \text{if } \hat{z}_2^+ \le d_n \le \hat{z}_2^- \\ \hat{z}_2^- & \text{if } d_n > \hat{z}_2^- \end{cases} ,$$

$$\kappa_n := \begin{cases} U^- & \text{if } \gamma_n \le 0 \\ U^+ & \text{if } \gamma_n > 0 \end{cases} ,$$

$$m_n := \left\lfloor \tfrac{1}{2} + \sqrt{\tfrac{1}{4} + 2\left|\tfrac{\gamma_n}{\kappa_n}\right|} \right\rfloor .$$

and where $\lceil\cdot\rceil$ and $\lfloor\cdot\rfloor$ respectively return the ceil and the floor of their arguments.

2) Surface σ_3

$$\sigma_3 := -\tfrac{2}{h(h+\tau)} z_1 - \tfrac{2h+\tau-1}{h(h+\tau)} z_2 - \tfrac{\tau(1-\tau^2)}{6h(h+\tau)}\alpha - \tfrac{2h^3-3h^2+h+3h^2\tau-3h\tau}{6h(h+\tau)}\beta , \tag{15}$$

where

$$[\alpha \ \beta] := \begin{cases} [U^- \ U^+] & \text{if } \eta = 1 \\ [U^+ \ U^-] & \text{if } \eta = -1 \end{cases} , \tag{16}$$

while $h, \tau \in \mathbb{N}^+$ and $\eta = \pm 1$ are parameters that depend on z_1 and z_2. The role and the meaning of such parameters will be discussed in Section III. The procedure that is used to devise σ_3 is proposed in the same section.

3) Surface σ_4

$$\sigma_4 := \frac{n_1 \ \alpha + n_2 \ \beta + n_3 \ z_1 + n_4 \ z_2}{6 \ d_1} , \tag{17}$$

where

$$\begin{aligned} n_1 &:= 6\left[j^2 + \hat{\tau}(\hat{\tau}-1) + (2\hat{\tau}-1)j\right]\hat{\rho}^2 \\ &\quad + 2\hat{\tau}\hat{\rho}\left[6j^2 + 9j(\hat{\tau}-1) + 2\hat{\tau}^2 + 1 - 9\hat{\tau}\right] \\ &\quad + 6\left[j^2 + (\hat{\tau}-2)j\right]\hat{\tau}^2 + \hat{\tau}^4 - 6\hat{\tau}^3 + 5\hat{\tau}^2 , \\ n_2 &:= 6h(1-h)(j\hat{\rho} + \hat{\rho}\hat{\tau} + j\hat{\tau}) - 2\hat{\rho}h(2 - 3h + h^2) \\ &\quad - h\hat{\tau}(7 - 9h + 2h^2) + 3\hat{\tau}^2 h(1-h) , \\ n_3 &:= -12(\hat{\tau} + \hat{\rho}) , \\ n_4 &:= -12(h+j)(\hat{\tau} + \hat{\rho}) + 12\hat{\rho}(1-\hat{\tau}) + 6\hat{\tau}(3-\hat{\tau}) , \\ d_1 &:= h\left[\hat{\tau}(\hat{\tau} - 2 + h + 2j) + \hat{\rho}(2j - 1 + h + 2\hat{\tau})\right] , \end{aligned}$$

and where α and β are defined according to (16), while $\hat{\tau}$ and $\hat{\rho}$ are evaluated by means of the following expressions

$$z^* := \begin{cases} z_3^+ & \text{if } \eta = 1 \\ z_3^- & \text{if } \eta = -1 \end{cases} , \tag{18}$$

$$\hat{\tau} := \left\lfloor -\tfrac{z^*}{\alpha} \right\rfloor , \tag{19}$$

$$\hat{\rho} := -\tfrac{z^*}{\alpha} - \hat{\tau} . \tag{20}$$

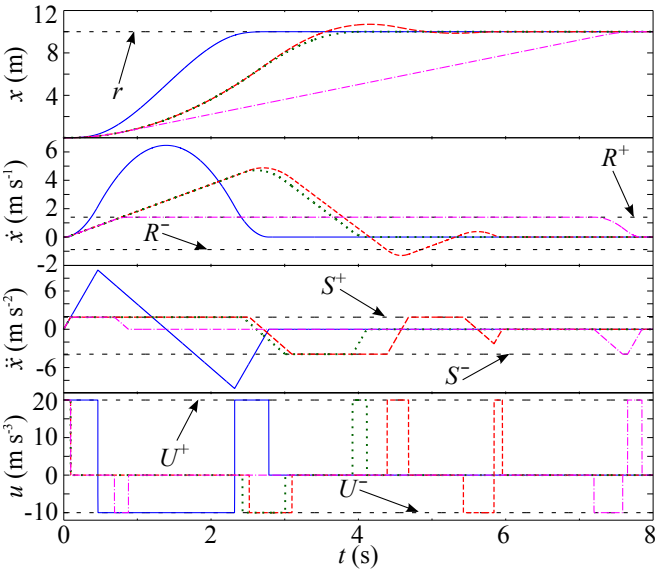

Fig. 3. Comparison between transients that are achived by using σ_3 (solid lines), σ_3, σ_5, and σ_6 (dashed lines), σ_3, σ_4, σ_5, and σ_6 (dotted lines), all the SSs (dash-dotted lines).

Parameters $h, j \in \mathbb{N}^+$, and $\eta = \pm 1$ only depend on z_1 and z_2. Their role and meaning will be discussed in §IV, together with the method that is used to devise σ_4. It is worth to point out that, because of (18)–(20), $\hat{\rho} \in [0, 1)$, while $\hat{\tau} \in \mathbb{N}^+$.

4) Surfaces σ_5 and σ_6

$$\sigma_5 := z_3^+ , \tag{21}$$

$$\sigma_6 := z_3^- . \tag{22}$$

Let us explain the role of each SS by means of the simple rest-to-rest transient that is shown in Fig. 3. The following limits have been assumed: $U^- = -10$ m s^{-3}, $U^+ = 20$ m s^{-3}, $S^- = -3.9$ m s^{-2}, $S^+ = 1.9$ m s^{-2}, $R^- = -0.95$ m s^{-1}, and $R^+ = 1.4$ m s^{-1}. Surface σ_3 drives the system, in minimum time, compatibly with the jerk constraint, toward the origin. It does not account for the velocity and the acceleration limits, so that such bounds could be violated, as shown by the solid curves in Fig. 3. The fulfillment of the acceleration constraint can potentially be achieved by using σ_5 and σ_6 in any area of the (z_1, z_2)-space in which σ_3 is unfeasible. Indeed, z_3^+ and z_3^-, that are defined according to (12), represent the equivalent bounds, in the $\mathbf{z}$-space, of S^+ and S^-. The dashed transients in Fig. 3 highlight that this solution, that is similar to the one that was used in [28], has a drawback: An overshoot can appear. The filter will be used to generate reference signals for industrial machines, so that such overshoot is clearly undesired. Moreover, the transient is not minimum-time. Surface σ_4, when used in conjunction with σ_3, as shown by the dotted lines in Fig. 3, eliminates both issues. The last two surfaces, i.e., σ_1 and σ_2, are used to guarantee the fulfillment of the velocity limits: The dash-dotted lines in Fig. 3 correspond to the system response that is obtained when all the surfaces are simultaneously used.

The role and the convergence properties of all the surfaces will be deeper analyzed in the next sections.

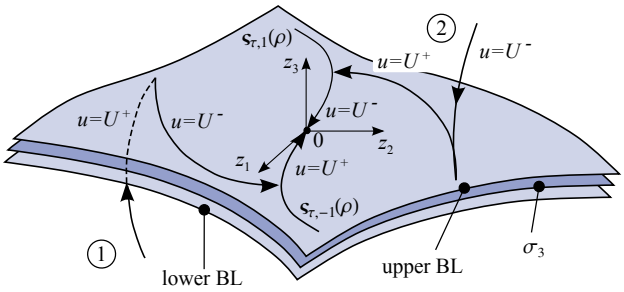

Fig. 4. Schematic representation of some transients toward the origin. Surface σ_3 is shown together with its BL.

III. Design and convergence properties of σ_3

Surface σ_3 is designed to drive the system state toward the origin in minimum time by fulfilling, at the same time, the jerk constraint. Differently from the SS that was proposed in [27], it is able to handle asymmetric jerk bounds. Let us consider a command law that only uses σ_3, i.e., let us control (6) by means of (8), (15), (16), and by assuming

$$\sigma = \sigma_3 \ . \tag{23}$$

Equations (15) and (16) determine the shape of σ_3, while (8) wraps the SS within an appropriate BL.

The optimality of the transients from any generic state $\mathbf{z}$ can be exploited with the aid of Fig. 4, that schematically shows two typical trajectories toward the origin. If the initial state is located below σ_3 (see Transient 1 in Fig. 4), the control law returns $u = U^+$, so that the z_3 component of $\mathbf{z}$, owing to (6) and (7), increases: σ_3 covers the whole (z_1, z_2)-space, so that the BL is certainly reached in minimum time. Once the state is inside the BL, command signal becomes, as it will soon be shown, $u = U^-$ and the state reaches curve $\varsigma_{\tau,\eta}(\rho)$ where a new switch occurs. The origin is finally approached with $u = U^+$. According to the Pontryagin's maximum principle, the transient is minimum-time, since u is bang-bang and two switches have occurred. Similar transients are obtained for initial states located above σ_3 (see Transient 2 in Fig. 4).

Let us describe the design of σ_3 and prove the optimality of the transients from any generic state $\mathbf{z}$ within the BL to the origin. First of all, it is possible to prove that all points $\mathbf{p}_{h,\tau,\eta}$, from which the origin can be reached in minimum time by means of a bang-bang command signal and with a single switch, have equation

$$\mathbf{p}_{h,\tau,\eta} = \begin{bmatrix} -\left[\frac{\tau(\tau-1)(\tau-2)}{6} + \frac{h\tau(h+\tau-2)}{2}\right]\alpha - \frac{h(h-1)(h-2)}{6}\beta \\ \left[\frac{\tau(\tau-1)}{2} + h\,\tau\right]\alpha + \frac{h(h-1)}{2}\,\beta \\ -\tau\,\alpha - h\,\beta \end{bmatrix} \tag{24}$$

where α and β, according to (16), depend on η. To this purpose, a first set of points, indicated in the following by $\mathbf{p}_{\tau,\eta}$, has been individuated by integrating backward system (6) from the origin. Two situations have been considered, each of them is denoted by a different value of η: If $\eta = 1$, then the system is driven with command signal $u = U^-$, while $u = U^+$ if $\eta = -1$. By means of this procedure, the following points have been obtained

$$\mathbf{p}_{\tau,\eta} = \begin{bmatrix} -\frac{\tau}{6}\left(\tau^2 - 3\tau + 2\right)\alpha & \frac{\tau}{2}\left(\tau - 1\right)\alpha & -\tau\,\alpha \end{bmatrix}^T ,$$

where α depends on η because of (16), while $\tau \in \mathbb{N}^+$ indicates the number of back integrations that have occurred. Evidently, from any point $\mathbf{p}_{\tau,\eta}$, the origin can be reached in minimum time with τ steps by applying the maximum admissible command signal, i.e., $u = U^-$ if $\eta = 1$ or $u = U^+$ if $\eta = -1$.

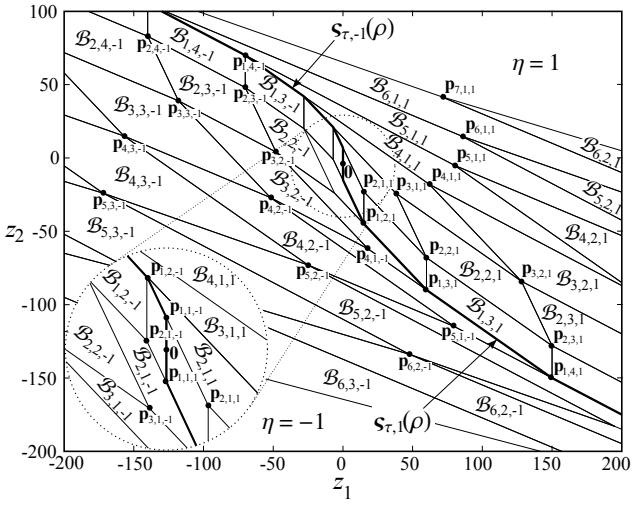

Fig. 5. Projection of σ_3 on the (z_1, z_2)-plane. Curve $\varsigma_{\tau,\eta}(\rho)$ separates the two zones that admit different values of η.

From any point $\mathbf{p}_{\tau,\eta}$ a new stage of backward integrations returns points $\mathbf{p}_{h,\tau,\eta}$ as defined by (24). They are obtained by switching the command signal, so that from points $\mathbf{p}_{\tau,-1}$ command signal $u = U^-$ is assumed while, viceversa, $u = U^+$ from points $\mathbf{p}_{\tau,1}$. Evidently, bearing in mind the definitions of α and β given by (16), from any point $\mathbf{p}_{h,\tau,\eta}$ the origin is reached, by construction, by first applying command signal $u = \beta$, for $h \in \mathbb{N}^+$ steps and, then, by assuming $u = \alpha$ for $\tau \in \mathbb{N}^+$ steps. The control is clearly bang-bang, a single switch occurs, so that it is possible to assert that the transient toward the origin is, according to the Pontryagin's maximum principle, minimum-time.

Points $\mathbf{p}_{h,\tau,\eta}$, as shown in Fig. 5, completely cover the (z_1, z_2)-space, that is partitioned into two sectors depending on η. The borderline between the two sectors is given by curve $\varsigma_{\tau,\eta}(\rho)$. The vertexes of σ_3 are obtained by adding vector $[0\ 0\ \beta]^T$ to points $\mathbf{p}_{h,\tau,\eta}$. σ_3 is a composite SS that is made of flat quadrangles and that, evidently, covers the whole (z_1, z_2)-plane. Each quadrangle is indexed by h, τ, η. Given any point in the (z_1, z_2)-plane, the corresponding value of σ_3 is found by first individuating the quadrangle h, τ, η in which it is located – to this purpose, techniques similar to those proposed in [35] can be adopted – and, then, by using (15) and (16).

Equations (8), (15), (16), and (23) associate to each point $\mathbf{p}_{h,\tau,\eta}$ a planar sliding surface σ_3 and its BL. In particular, as shown in Fig. 6, a box $\mathcal{B}_{h,\tau,\eta}$, which upper/lower surfaces are given by the borders of the BL, is associated to each point

$\mathbf{p}_{h,\tau,\eta}$. $\mathcal{B}_{h,\tau,\eta}$ can be formally defined as follows

$$\mathcal{B}_{h,\tau,\eta} := \{\mathbf{z} : \mathbf{z} = \mathbf{p}_{h,\tau,\eta} + \lambda\,\bar{\mathbf{e}}_{h,\tau,\eta} + \mu\,\tilde{\mathbf{e}}_{h,\tau,\eta} + \nu\,\hat{\mathbf{e}}_{h,\tau,\eta}; \lambda,\mu,\nu \in [0,1)\} \quad (25)$$

where $\mathbf{p}_{h,\tau,\eta}$ is given by (24), while vectors $\bar{\mathbf{e}}_{h,\tau,\eta}$, $\tilde{\mathbf{e}}_{h,\tau,\eta}$, and $\hat{\mathbf{e}}_{h,\tau,\eta}$ are defined as follows

$$\bar{\mathbf{e}}_{h,\tau,\eta} := \alpha\left[-\tfrac{1}{2}\left[\tau(\tau-1)+h(h-1)+2h\tau\right] \quad h+\tau \quad -1\right]^T, \quad (26)$$

$$\tilde{\mathbf{e}}_{h,\tau,\eta} := (\alpha-\beta)\left[\tfrac{1}{2}\,h(h-1) \quad -h \quad 1\right]^T, \quad (27)$$

$$\hat{\mathbf{e}}_{h,\tau,\eta} := [0 \;\; 0 \;\; \beta-\alpha]^T. \quad (28)$$

The vectors placement is shown in Fig. 6 for $\eta = 1$. Practically, vectors (26)–(28) represent a non-orthogonal reference frame that can be used to describe any point $\mathbf{z} \in \mathcal{B}_{h,\tau,\eta}$. More precisely, any point $\mathbf{z} \in \mathcal{B}_{h,\tau,\eta}$ can be alternatively represented by means of a vector of six elements $\bar{\mathbf{z}} := [h\ \tau\ \eta\ \lambda\ \mu\ \nu]^T$: The first three coordinates individuate the box, the last three define the position inside the box. In this representation, the origin assumes coordinates $\bar{\mathbf{z}} := [1\ 1\ \eta\ 0\ \frac{-\alpha}{\beta-\alpha}\ \frac{\beta}{\beta-\alpha}]^T$.

Bearing in mind these premises, it is possible to prove the optimality of the transients from any point that is located inside the BL. In particular, from any initial state $\mathbf{z}_0 \in \mathcal{B}_{h,\tau,\eta}$ or, equivalently, from $\bar{\mathbf{z}}_0 = [h\ \tau\ \eta\ \lambda\ \mu\ \nu]^T$, with $h,\tau \in \mathbb{N}^+$, the origin is certainly reached, if system (6) is controlled by means of (8), (15), (16), and (23), according to the following sequence of steps:

i	$\bar{\mathbf{z}}_i$	u_{i+1}
0	$[h\ \tau\ \eta\ \lambda\ \mu\ \nu]^T$	$\nu\alpha + (1-\nu)\beta$
1	$[(h-1)\ \tau\ \eta\ \lambda\ \mu\ 0]^T$	β
2	$[(h-2)\ \tau\ \eta\ \lambda\ \mu\ 0]^T$	β
$\vdots$		β
$h-1$	$[1\ \tau\ \eta\ \lambda\ \mu\ 0]^T$	β
h	$[1\ (\tau-1)\ \eta\ \lambda\ 0\ (1-\mu)]^T$	$\mu\beta + (1-\mu)\alpha$
$h+1$	$[1\ (\tau-2)\ \eta\ \lambda\ 0\ 1]^T$	α
$\vdots$		α
$h+\tau-2$	$[1\ 1\ \eta\ \lambda\ 0\ 1]^T$	α
$h+\tau-1$	$[1\ 1\ \eta\ 0\ \frac{\alpha(\lambda-1)}{\beta-\alpha}\ 1]^T$	α
$h+\tau$	$[1\ 1\ \eta\ 0\ \frac{-\alpha}{\beta-\alpha}\ \frac{\beta-\lambda\alpha}{\beta-\alpha}]^T$	$\lambda\alpha$
$h+\tau+1$	$[1\ 1\ \eta\ 0\ \frac{-\alpha}{\beta-\alpha}\ \frac{\beta}{\beta-\alpha}]^T$	

Evidently, $h+\tau+1$ steps are required, i.e., only one more step with respect to the optimal transient from $\mathbf{p}_{h,\tau,\eta}$. According to the Pontryagin's maximum principle, a single switch occurs and the command signal, apart from switching instants, is always equal to β or to α, i.e., by virtue of (16), it is equal to U^+ or to U^-. It is worth to point out that, at the switching instants, the command signal cannot be exactly equal to β or α because the switching times of discrete-time systems are fixed and cannot be freely selected. If the initial state is equal to $\mathbf{p}_{h,\tau,\eta}$, i.e., $\bar{\mathbf{z}}_0 = [h\ \tau\ \eta\ 0\ 0\ 0]^T$, the sequence converges to the origin in $h+\tau$ steps and u is, as desired, exactly bang-bang.

IV. Design and Convergence Properties of σ_4

Surface σ_3 manages neither the velocity nor the acceleration constraints that, consequently, could be violated. The acceleration constraint could potentially be satisfied by simply bounding the third component of $\mathbf{z}$ within interval $[z_3^+, z_3^-]$. It was early anticipated that this result can be achieved by adopting σ_3 only in the areas of the (z_1, z_2)-space in which it is feasible, and by using σ_5 and σ_6 in the other zones. As shown in Section II, this rough approach can cause overshoots and suboptimal transients. For this reason, in any zone of the (z_1, z_2)-plane in which σ_3 would lead to unfeasible accelerations, an alternative surface σ_4 is used.

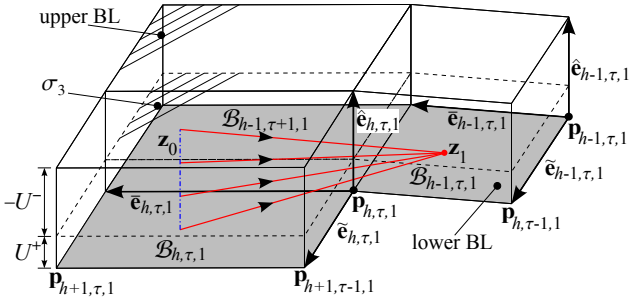

Fig. 6. Single-step evolution starting from box $\mathcal{B}_{h,\tau,1}$.

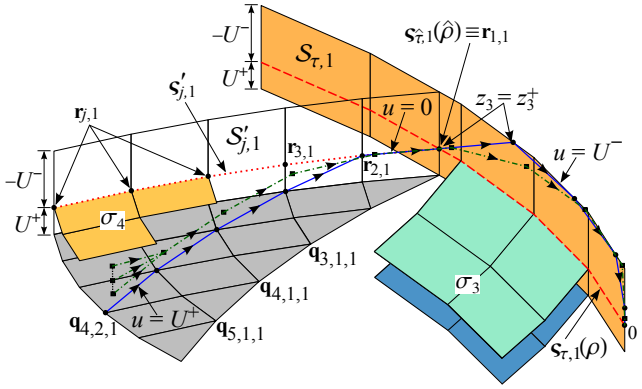

Fig. 7. 3D view of a transient toward the origin for $\eta = 1$ starting from $\mathbf{q}_{2,4,1}$ (solid line) and from a generic point inside the BL (dash-dotted line). Point $\varsigma_{\hat{\tau},1}(\hat{\rho})$ is reached in 5 steps, then the origin is gained by means of σ_3. The same number of steps is required for the second transient. Upper bound z_3^+ is never violated.

Surface σ_4, similarly to σ_3, has been planned by first individuating a set of points $\mathbf{q}_{h,j,\eta}$ from which the origin can be reached in minimum time by means of a trajectory that fulfills both the jerk and the acceleration constraints. The positions of such points are given by (29). The Pontryagin's maximum principle suggests that, because of the additional constraint, optimal transients must be bang-zero-bang. Fig. 7, which shows a situation in which $\eta = 1$, can be used to explain the synthesis of σ_4. By integrating backward from the origin system (6), with $u = U^-$, a monotonically increasing curve is obtained. An indefinite execution of the back integration process would clearly lead to the violation of upper bound z_3^+. In order preserve feasibility, in proximity of z_3^+ the command signal is switched to $u = 0$, and a set of points $\mathbf{r}_{j,1}$ is obtained. They are characterized by a third component equal to z_3^+, i.e., they are all strictly feasible with respect to the acceleration bound. Points $\mathbf{q}_{h,j,1}$ are finally obtained by means of a new stage of back integrations from $\mathbf{r}_{j,1}$, which

$$\mathbf{q}_{h,j,\eta} = \begin{bmatrix} \alpha\left\{-\frac{\hat{\tau}^3}{6} - \frac{(h+j+\hat{\rho}-2)\hat{\tau}^2}{2} + \frac{\left[6(h+j)(2-\hat{\rho})-3(h+j)^2+9\hat{\rho}-11\right]\hat{\tau}}{6} + \frac{\left[(3-2h)j-j^2-(h-1)(h-2)\right]\hat{\rho}}{2}\right\} - \frac{\beta h}{6}(h-1)(h-2) \\ \alpha\left[\frac{1}{2}\hat{\tau}(\hat{\tau}-3) + (j+\hat{\tau}+h-1)\hat{\rho} + \hat{\tau}(h+j)\right] + \frac{1}{2}\beta h(h-1) \\ -\alpha(\hat{\tau}+\hat{\rho}) - \beta h \end{bmatrix}, \quad (29)$$

is made by assuming $u = U^+$. An analogous sequence of backward integrations is used for $\eta = -1$ in order to devise points $\mathbf{q}_{h,j,-1}$, but in this second case the command sequence becomes $u = U^+ \Rightarrow u = 0 \Rightarrow u = U^-$.

Fig. 7 also shows a typical approach to the origin from $\mathbf{q}_{4,2,1}$ ($h = 4$, $j = 2$, $\eta = 1$). If system (6) is driven with $u = U^+$, point $\mathbf{r}_{2,1}$ is reached after h steps (in the example $h = 4$). The transient is clearly minimum-time because the maximum available jerk has been used. As previously mentioned, points $\mathbf{r}_{j,1}$ are characterized, by construction, by a third component, equal to z_3^+, i.e., equal to the maximum allowable acceleration. Evidently, all points along curve $\boldsymbol{\varsigma}'_{j,1}$, which passes through points $\mathbf{r}_{j,1}$, possess the same property. In $\mathbf{r}_{2,1}$, command signal switches to $u = 0$ in order to avoid the violation of the acceleration bound, and the state slides along $\boldsymbol{\varsigma}'_{j,1}$ toward $\boldsymbol{\varsigma}_{\hat{\tau},1}(\hat{\rho})$ that is reached with further $j-1$ steps (in the example $j = 2$, thus a single step is required). The transient is again minimum-time, since $u = 0$ is the maximum allowable command signal which guarantees the feasibility.

From $\boldsymbol{\varsigma}_{\hat{\tau},1}(\hat{\rho})$, the origin is finally gained in $\hat{\tau}+2$ steps ($\hat{\tau}+1$ if $\hat{\rho} = 0$) with $u = U^-$. It is possible to prove that this final transient exactly coincides with the final transient that can be obtained by means of σ_3, so that the actual implementation of the control law uses σ_3 for the final convergence to the origin. In conclusion, from any point $\mathbf{q}_{h,j,\eta}$, the origin is reached after $h + j + \hat{\tau} + 1$ steps ($h + j + \hat{\tau}$ if $\hat{\rho} = 0$) by means of a bang-zero-bang command signal and by fulfilling the acceleration constraint. The transient is clearly time-optimal.

Vertexes of surface σ_4 are obtained by adding $[0 \;\; 0 \;\; \beta]^T$ to points $\mathbf{q}_{h,j,\eta}$. By construction, for $\eta = 1$, σ_4 monotonically decreases in function of h and, moreover, $\sigma_4 \leq z_3^+$, i.e., it is feasible with respect to the upper acceleration constraint. On the contrary, for $\eta = -1$, σ_4 monotonically increases in function of h and $\sigma_4 \geq z_3^-$.

By assuming a command law given by (8), (16), (17), and

$$\sigma = \sigma_4 \; , \quad (30)$$

a BL is created around σ_4. In the following it is shown that, by means of such control law, the origin is reached in minimum time from any generic state $\mathbf{z}$ that is located inside the BL. Similarly to σ_3, surface σ_4 attracts the system state with a command signal that is equal to U^+ or U^-, i.e., in minimum time. The transient toward the origin starts after the BL of σ_4 has been reached. Let us prove its optimality and feasibility. Command law (8), (16), (17), and (30) associates, to each point $\mathbf{q}_{h,j,\eta}$, a box $\mathcal{W}_{h,j,\eta}$ which upper and lower surfaces coincide with the BL limits and that is formally defined as follows

$$\mathcal{W}_{h,j,\eta} := \left\{\mathbf{z} : \mathbf{z} = \mathbf{q}_{h,j,\eta} + \lambda\bar{\mathbf{e}}'_{h,j,\eta} + \mu\tilde{\mathbf{e}}'_{h,j,\eta} + \nu\hat{\mathbf{e}}'_{h,j,\eta}; \; \lambda,\mu,\nu \in [0,1)\right\} \quad (31)$$

where

$$\bar{\mathbf{e}}'_{h,j,\eta} := \begin{bmatrix} (-h-\hat{\tau}-j+1)\hat{\rho} - \hat{\tau}(\frac{1}{2}\hat{\tau}+h+j-\frac{3}{2}) \\ \hat{\tau}+\hat{\rho} \\ 0 \end{bmatrix} \alpha, \quad (32)$$

$$\tilde{\mathbf{e}}'_{h,j,\eta} := \left[-\tfrac{1}{2}\,h\,(h-1)\beta \;\; h\beta \;\; -\beta\right]^T , \quad (33)$$

$$\hat{\mathbf{e}}'_{h,j,\eta} := [0 \;\; 0 \;\; \beta-\alpha]^T . \quad (34)$$

Bearing in mind (29)–(34), any point $\mathbf{z} \in \mathcal{W}_{h,j,\eta}$ can be alternative represented as $\hat{\mathbf{z}} := [h \; j \; \eta \; \lambda \; \mu \; \nu]^T$.

The optimality of the transients that are obtained by means of σ_4 is proved by verifying that, from any state $\mathbf{z} \in \mathcal{W}_{h,j,\eta}$, the origin is reached in $h+j+\hat{\tau}+1$ steps, i.e., the same number of steps that are required from $\mathbf{q}_{h,j,\eta}$ with the minimum-time control, and that u is bang-zero-bang. In particular, by adopting command law (8), (16), (17), and (30), system (6) evolves, from any initial state $\mathbf{z}_0 \in \mathcal{W}_{h,j,\eta}$, with $h, j \in \mathbb{N}^+$ or, equivalently, from $\hat{\mathbf{z}}_0 = [h \; j \; \eta \; \lambda \; \mu \; \nu]^T$, as follows:

i	$\hat{\mathbf{z}}_i$	u_{i+1}
0	$[h \; j \; \eta \; \lambda \; \mu \; \nu]^T$	$\nu\alpha + (1-\nu)\beta$
1	$[(h-1) \; j \; \eta \; \lambda \; \mu \; 0]^T$	β
2	$[(h-2) \; j \; \eta \; \lambda \; \mu \; 0]^T$	β
$\vdots$		β
$h-1$	$[1 \; j \; \eta \; \lambda \; \mu \; 0]^T$	β
h	$[1 \; (j-1) \; \eta \; \lambda \; 0 \; \frac{(1-\mu)\beta}{\beta-\alpha}]^T$	$\mu\beta$
$h+1$	$[1 \; (j-2) \; \eta \; \lambda \; 0 \; \frac{\beta}{\beta-\alpha}]^T$	0
$\vdots$		0
$h+j-2$	$[1 \; 1 \; \eta \; \lambda \; 0 \; \frac{\beta}{\beta-\alpha}]^T$	

The transient is also shown by the dash-dotted line of Fig. 7, for $\eta = 1$. Practically, with a single step the state is projected on the lower surface of the BL. At step $h-1$, $\mathbf{z}$ reaches box $\mathcal{W}_{1,j,\eta}$, then, with a single step, it moves on the lateral surface $\mathcal{S}'_{j-1,\eta}$ of $\mathcal{W}_{1,j-1,\eta}$. It is possible to verify that points lying on $\boldsymbol{\varsigma}'_{j,\eta}$ have equation $[1 \; j \; \eta \; \lambda \; 0 \; \frac{\beta}{\beta-\alpha}]^T$, so that $\mathbf{z}_h$ is clearly located below $\boldsymbol{\varsigma}'_{j-1,\eta}$ when $\eta = 1$ (or above $\boldsymbol{\varsigma}'_{j-1,\eta}$ if $\eta = -1$), while the subsequent state, i.e., $\mathbf{z}_{h+1}$, exactly lies on $\boldsymbol{\varsigma}'_{j-2,\eta}$. Box $\mathcal{W}_{1,1,\eta}$ is reached, after $h + j - 2$ steps with $u = 0$ and with an acceleration that is equal to z^*, i.e., to z_3^+ or to z_3^- depending on η: The whole transient is feasible with respect to the acceleration constraint.

The subsequent step is the most critical. It was early anticipated that the final transient toward the origin is achieved by means of σ_3: The state, with a single transient, enters in the area that is handled by such SS. As shown in Fig. 8, two alternative situations can arise depending on $\hat{\rho}$, both characterized by $u = 0$:

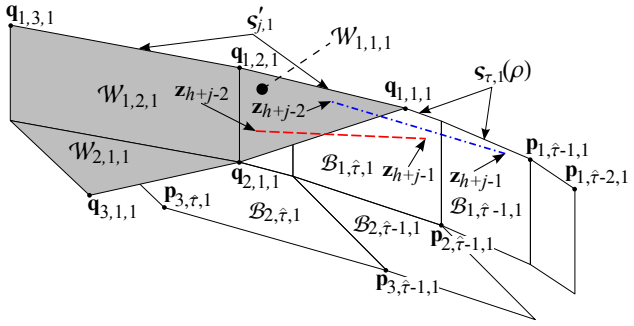

Fig. 8. 2D view in the (z_1, z_2)-space of the switching phase between σ_4 and σ_3 ($\eta = 1$). Starting from $\mathcal{W}_{1,1,1}$ the state always reaches, with a single step, $\mathcal{B}_{1,\hat{\tau},1}$ (dashed line) or $\mathcal{B}_{1,\hat{\tau}-1,1}$ (dash-dotted line).

a) $\hat{\rho} \geq [(1-\lambda)(\hat{\tau}-1)]/[\hat{\tau}+2\lambda-1]$. The state evolves to $\bar{\mathbf{z}}_{h+j-1} = [1\ \hat{\tau}\ \eta\ a_1\ a_2\ a_3]^T$ where $a_1 = [(\lambda-1)(\hat{\tau}-1) + \hat{\rho}(\hat{\tau}+2\lambda-1)]/(\hat{\tau}+1)$, $a_2 = [(1-\hat{\rho})(\lambda-1)\alpha]/(\beta-\alpha)$, and $a_3 = \{\beta(\hat{\tau}+1)+\alpha[\hat{\tau}(\lambda-1)(2-\hat{\rho})+\hat{\rho}(\lambda-1)]\}/[(\hat{\tau}+1)(\beta-\alpha)]$. It is easy to verify that coefficients $a_1, a_2, a_3 \in [0,1)$, so that $\mathbf{z}_{h+j-1} \in \mathcal{B}_{1,\hat{\tau},\eta}$;

b) $\hat{\rho} < [(1-\lambda)(\hat{\tau}-1)]/[\hat{\tau}+2\lambda-1]$. The state evolves to $\bar{\mathbf{z}}_{h+j-1} = [1\ (\hat{\tau}-1)\ \eta\ a_1\ a_2\ a_3]^T$ where $a_1 = [\hat{\rho}(\hat{\tau}-1) + \lambda(\hat{\tau}+2\hat{\rho}-1)]/(\hat{\tau}-1)$, $a_2 = -[\alpha\lambda\hat{\rho}(\hat{\tau}+1)]/[(\hat{\tau}-1)(\beta-\alpha)]$, and $a_3 = [\beta-\alpha(1-\lambda+\lambda\hat{\rho})]/(\beta-\alpha)$. Coefficients $a_1, a_2, a_3 \in [0,1)$, so that $\mathbf{z}_{h+j-1} \in \mathcal{B}_{1,\hat{\tau}-1,\eta}$.

Once inside $\mathcal{B}_{1,\hat{\tau},\eta}$, the origin is reached with σ_3 according to the following steps (one less step is required from $\mathcal{B}_{1,\hat{\tau}-1,\eta}$):

i	$\bar{\mathbf{z}}_i$	u_{i+1}
$h+j-1$	$[1\ \hat{\tau}\ \eta\ a_1\ a_2\ a_3]^T$	$a_3\alpha + (1-a_3)\beta$
$h+j$	$[1\ (\hat{\tau}-1)\ \eta\ a_1\ 0\ (1-a_2)]^T$	$a_2\beta + (1-a_2)\alpha$
$h+j+1$	$[1\ (\hat{\tau}-2)\ \eta\ a_1\ 0\ 1]^T$	α
$\vdots$		α
$h+j+\hat{\tau}-2$	$[1\ 1\ \eta\ a_1\ 0\ 1]^T$	α
$h+j+\hat{\tau}-1$	$[1\ 1\ \eta\ 0\ \frac{\alpha(a_1-1)}{\beta-\alpha}\ 1]^T$	α
$h+j+\hat{\tau}$	$[1\ 1\ \eta\ 0\ \frac{-\alpha}{\beta-\alpha}\ \frac{\beta-a_1\alpha}{\beta-\alpha}]^T$	$a_1\alpha$
$h+j+\hat{\tau}+1$	$[1\ 1\ \eta\ 0\ \frac{-\alpha}{\beta-\alpha}\ \frac{\beta}{\beta-\alpha}]^T$	

Thus, starting from any state $\mathbf{z}_0 \in \mathcal{W}_{j,h,\eta}$, the origin is reached, in the worst case, in $h+j+\hat{\tau}+1$ steps, i.e., the same number of steps of the transients that are required from $\mathbf{q}_{j,h,\eta}$. The transient optimality is also proved by the bang-zero-bang behavior of the command signal, that admits $u = 0$ only when the acceleration is equal to the maximum admissible value.

V. Convergence properties of σ_1 and σ_2

Surfaces σ_1 and σ_2 are used to fulfill the velocity limits. To this aim, they force $\mathbf{z}$ inside the quadrangle that is shown in Fig. 9 and that has been obtained by converting the feasible domain of the $(\dot{x}, \ddot{x})$-space – that is represented by a rectangle that is bounded by the following four straight lines: $\ddot{x} = S^+$, $\ddot{x} = S^-$, $\dot{x} = R^+$, and $\dot{x} = R^-$ – into an equivalent feasible domain in the (z_2, z_3)-space.

Surfaces σ_1 and σ_2 are derived from an analogous surface that was originally proposed in [36]. This is possible because

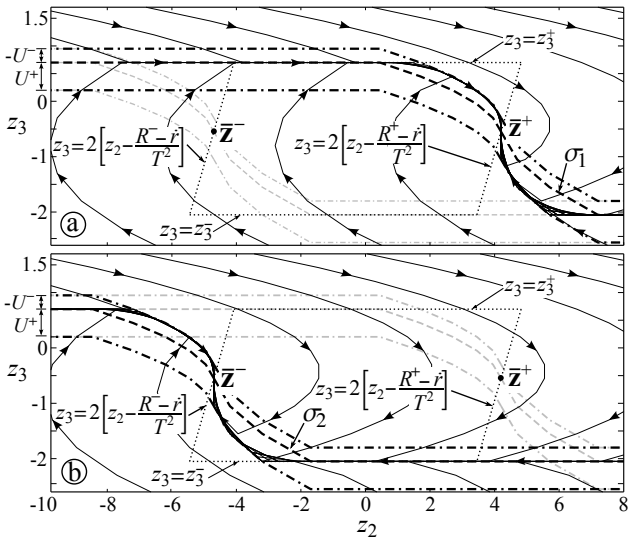

Fig. 9. System trajectories in the (z_2, z_3)-space obtained by assuming: a) $\sigma = \sigma_1$ and b) $\sigma = \sigma_2$. SSs σ_1 and σ_2 are indicated by means of dashed lines and are surrounded by their BLs (dash dotted lines). The dotted quadrangle contours the feasible area. z_3^+ and z_3^- are defined according to (12).

the evolution of system (6) in the (z_2, z_3)-space does not depend on the z_1 component of the state and it is given by

$$\begin{bmatrix} z_{2,i+1} \\ z_{3,i+1} \end{bmatrix} = \begin{bmatrix} 1 & 1 \\ 0 & 1 \end{bmatrix} \begin{bmatrix} z_{2,i} \\ z_{3,i} \end{bmatrix} + \begin{bmatrix} 1 \\ 1 \end{bmatrix} u_i \ ,$$

i.e., system equations coincide with those that were considered in [36], but the role of the pair z_1 and z_2 is now played by z_2 and z_3. Thus, by adopting the same command law that was proposed in [36], the same convergence properties are obtained. However, minor changes have been introduced in σ_1 and σ_2 in order to modify the convergence points: σ_1 guarantees the convergence toward $\bar{\mathbf{z}}^+$, while σ_2 guarantees the convergence toward $\bar{\mathbf{z}}^-$. Due to the lack of space, the convergence properties of σ_1 and σ_2 are here not analyzed, but they can be studied with the same methods that were considered in [36]. Conversely, it is interesting to analyze the state transients that are obtained when they are used. Fig. 9 shows the two SSs together with the corresponding BLs, the feasible area, and some system trajectories. All trajectories enter, independently from the selected SS, inside the feasible area. This result is achieved in minimum time because outside the BLs the command signal always assumes its maximum value, i.e., $u = U^+$ or $u = U^-$. Inside the BL, the state slides toward $\bar{\mathbf{z}}^+$ or $\bar{\mathbf{z}}^-$, that are respectively defined by (13) and (14): Such two points are the projections, in the (z_2, z_3)-space, of the homologous points $(R^+, 0)$ and $(R^-, 0)$ of the $(\dot{x}, \ddot{x})$-space, i.e., of the two state configurations in which the system assumes the maximum feasible speed with zero acceleration.

The role of such two points can be understood by analyzing a generic transient from a totally unfeasible state. According to *Problem* 1, feasibility must be achieved before any transient toward the origin could start. The jerk constraint is fulfilled with a single step due to (8), then the state is driven toward σ by applying the maximum command signal: Since σ_1, σ_2, and $\bar{\sigma}$ are all feasible with respect to the acceleration constraint, such constraint is fulfilled in minimum time independently

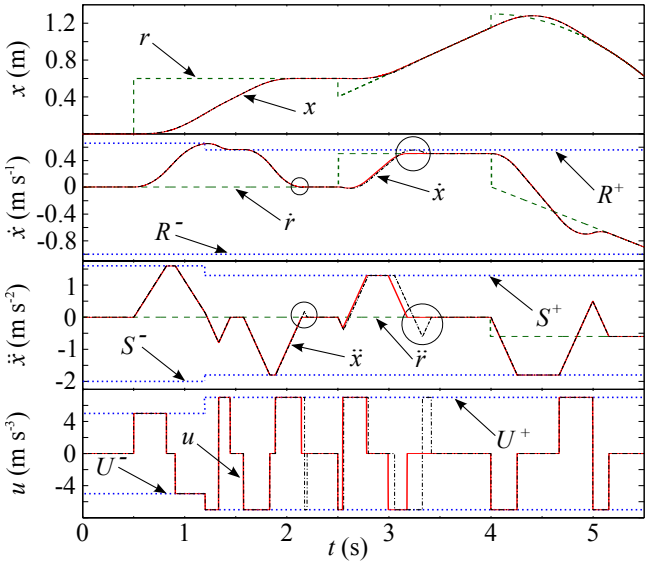

Fig. 10. Comparison between the outputs of the novel filter (solid lines) and those of the filter proposed in [28] (dash-dotted lines): Reference signal (dashed lines) is reached in minimum-time and by fulfilling the imposed bounds (dotted lines). Circles highlight the configurations for which the new filter returns shorter transients.

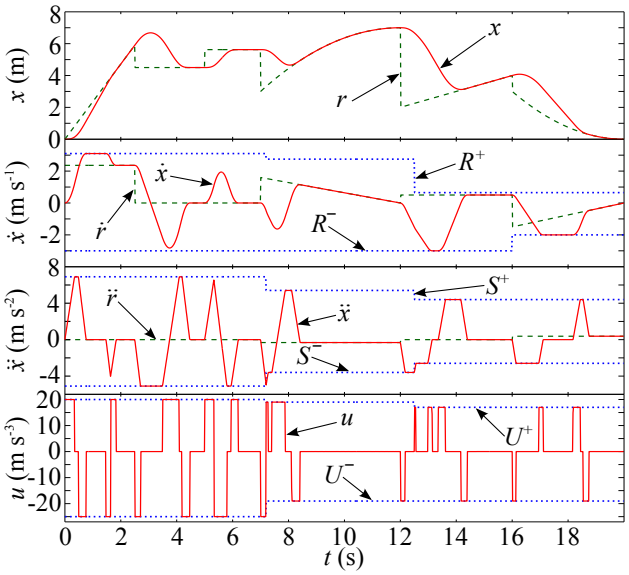

Fig. 11. Results of the second test case. The reference signal (dashed line) is tracked at the best by the filter output (solid lines). Given constraints are always satisfied (dotted lines).

from the choice that is made in (9). Subsequently, if $\overline{\sigma}$ should drive the system to violate the velocity bounds, σ_1 or σ_2 are used to "park" the state, in minimum time, in $\overline{\mathbf{z}}^-$ or $\overline{\mathbf{z}}^+$, i.e., in the two points corresponding to states $(R^-, 0)$ and $(R^+, 0)$ of the $(\dot{x}, \ddot{x})$-space: It is possible to demonstrate that, in those two points, the state moves at the maximum velocity, i.e., $\dot{x} = R^+$ or $\dot{x} = R^-$, toward $\overline{\sigma}$, to finally converge to the origin in minimum time with a feasible trajectory. The demonstration is similar to that proposed in [28] and is omitted for conciseness.

VI. A TEST CASE

In the first test case here proposed, the performances of the new filter are compared with those an analogous filter devised in [28]. As claimed in the Introduction, the new filter eliminates a suboptimal behavior that was affecting the version proposed in [28]: Depending on the reference signal and on the bounds, transients of [28] could be non-minimum-time and undesired overshoots could appear. The circles of Fig. 10 show two cases in which the new filter returns better solutions. Improvements are especially evident for the second of the two transients, which has been shortened by 0.3 s and its hanging overshoot has been eliminated. It is interesting to note that the transient toward the parabolic reference admits an overshoot in both approaches. This implies that the solution found in [28] was already minimum-time compatibly with the constraints: The overshoot can only be eliminated by loosening the bounds.

The second example tests the filter performances in case of asymmetric constraints, by using an input signal that is appositely devised in order to highlight the system capabilities. The test has been executed on a real-time system, based on RTAI [37]. As shown in Fig. 11, the reference signal is discontinuous and it is given by a combination of steps, ramps and parabolas. Assigned constraints are online changed. The filter, as expected, mimics the input signal by means of an output that fulfills the given velocity, acceleration, and jerk constraints. The reference signal is always reached without overshoot even when, at times $t = 7.2$ s and $t = 12.5$ s, the bounds are changed in the middle of a transient. Transients are always minimum time compatibly with the constraints. The jerk has a bang-zero-bang behavior and the chattering phenomenon is totally avoided. The filter has been executed with a sampling time $T = 1\text{e-}3$ s. An average evaluation time of 5.24e-6 s has been measured on a PC equipped with an Intel Core2 Duo processor @3GHz: Even considering less efficient processors, the computational burden would still be compatible with the sampling times of many industrial applications.

VII. CONCLUSIONS

The proposed filter is able to generate smooth reference signals starting from piecewise continuous inputs. Candidate applications of the novel system coincide with those that were proposed in [18]–[23]: With a moderate increment of the computational burden, the smoothness of the reference signals can be significantly improved.

Among the other properties of the algorithm, it is worth to mention its compactness and efficiency, which permit implementations based on commercial control-boards.

REFERENCES

[1] C.-S. Lin, P.-R. Chang, and J. Luh, "Formulation and optimization of cubic polynomial joint trajectories for industrial robots," *IEEE Trans. Automatic Control*, vol. AC-28, no. 12, pp. 1066–1074, 1983.

[2] A. De Luca, L. Lanari, and G. Oriolo, "A sensitivity approach to optimal spline robot trajectories," *Automatica*, vol. 27, no. 3, pp. 535–539, 1991.

[3] S. Macfarlane and E. A. Croft, "Jerk-bounded manipulator trajectory planning: design for real-time applications," *IEEE Trans. on Rob. and Autom.*, vol. 19, no. 1, pp. 42–52, 2003.

[4] L. Messner, H. Gattringer, and H. Bremer, "Efficient Online Computation of Smooth Trajectories Along Geometric Paths for Robotic Manipulators ," in *Multibody system dynamics, robotics, and control*, H. Gattringer and J. Gerstmayr, Eds. Wien: Springer-Verlag, 2013.
[5] K.-H. Rew and K.-S. Kim, "A Closed-Form Solution to Asymmetric Motion Profile Allowing Acceleration Manipulation ," *IEEE Trans on Ind. Electr.*, vol. 57, no. 7, pp. 2499–2506, July 2010.
[6] F. Zou, D. Qu, J. Wang, and F. Xu, "Asymmetric trajectory planning for vacuum robot motion," in *2011 IEEE Int. Conf.on Rob. and Autom., ICRA2011*, May 2011, pp. 1–4.
[7] C.-W. Ha, K.-H. Rew, and K.-S. Kim, "Robust Zero Placement for Motion Control of Lightly Damped Systems," *IEEE Trans. on Ind. Electr.*, vol. 60, no. 9, pp. 3857–3864, 2013.
[8] L. Biagiotti and C. Melchiorri, "FIR filters for online trajectory planning with time- and frequency-domain specifications," *Contr. Eng. Pract.*, vol. 20, no. 12, pp. 1385–1399, 2012.
[9] L. Rutkowski, A. Przybyl, and K. Cpalka, "Novel online speed profile generation for industrial machine tool based on flexible neuro-fuzzy approximation ," *IEEE Trans. on Ind. Electr.*, vol. 59, no. 2, pp. 1238–1247, Feb. 2012.
[10] R. Haschke, E. Weitnauer, and H. Ritter, "On-line planning of timeoptimal, jerk-limited trajectories," in *Proc. of the IEEE/RSJ Int. Conf. on Intelligent Robots and Systems, IROS 08*, 2008, pp. 3248–3253.
[11] T. Kröger and F. M. Wahl, "On-Line Trajectory Generation: Basic Concepts for Instantaneous Reactions to Unforeseen Events," *IEEE Trans. on Rob.*, vol. 26, no. 1, pp. 94–111, Feb. 2010.
[12] X. Broquère, D. Sidobre, and I. Herrera-Aguilar, "Soft motion trajectory planner for service manipulator robot," in *Proc. of the 2008 IEEE/RSJ Int. Conf. on Intell. Rob. and Systems, IROS 08*, 2008, pp. 2808–2813.
[13] C. Guarino Lo Bianco, A. Tonielli, and R. Zanasi, "Nonlinear trajectory generator for motion control systems," in *IECON96 - 22nd Int. Conf. of the IEEE Ind. Electr. Society*, Taiwan, Taipei, August 1996, pp. 195–201.
[14] X. Wei, J. Wang, and Z. Yang, "Robust Smooth-Trajectory Control of Nonlinear Servo Systems Based on Neural Networks," *IEEE Trans. Ind. Electr.*, vol. 54, no. 1, pp. 208–217, 2007.
[15] L. Biagiotti and R. Zanasi, "Online trajectory planner with constraints on velocity, acceleration and torque," in *Proc. of the IEEE Int. Symp. on Ind. Electr., ISIE2010*, Bari, Italy, Jul. 2010, pp. 274–279.
[16] C. Guarino Lo Bianco and R. Zanasi, "Smooth profile generation for a tile printing machine," *IEEE Trans. on Ind. Electr.*, vol. 50, no. 3, pp. 471–477, 2003.
[17] O. Gerelli and C. Guarino Lo Bianco, "Nonlinear variable structure filter for the online trajectory scaling," *IEEE Trans. on Ind. Electr.*, vol. 56, no. 10, pp. 3921–3930, Oct. 2009.
[18] B. Bona, M. Indri, and N. Smaldone, "Rapid prototyping of a model-based control with friction compensation for a direct-drive robot," *IEEE/ASME Trans. on Mechatr.*, vol. 11, no. 5, pp. 576–584, Oct. 2006.
[19] M. Montanari, S. Peresada, C. Rossi, and A. Tilli, "Speed sensorless control of induction motors based on a reduced-order adaptive observer," *IEEE Trans. on Contr. Sys. Tech.*, vol. 15, no. 6, pp. 1049–1064, 2007.
[20] E. Mininno, F. Neri, F. Cupertino, and D. Naso, "Compact differential evolution," *IEEE Trans. on Evol. Comp.*, vol. 15, no. 1, pp. 32–54, 2011.
[21] D. Naso, F. Cupertino, and B. Turchiano, "NPID and Adaptive Approximation Control of Motion Systems With Friction," *IEEE Trans. on Contr. Sys. Tech.*, vol. 20, no. 1, pp. 214–222, Jan. 2012.
[22] F. Cupertino, P. Giangrande, G. Pellegrino, and L. Salvatore, "End Effects in Linear Tubular Motors and Compensated Position Sensorless Control Based on Pulsating Voltage Injection ," *IEEE Trans. on Ind. Electr.*, vol. 58, no. 2, pp. 494–502, Feb. 2011.
[23] M. Corradini, V. Fossi, A. Giantomassi, G. Ippoliti, S. Longhi, and G. Orlando, "Minimal Resource Allocating Networks for Discrete Time Sliding Mode Control of Robotic Manipulators," *IEEE Trans. on Ind. Inf.*, vol. 8, no. 4, pp. 733–745, Nov. 2012.
[24] S. Liu, "An on-line reference-trajectory generator for smooth motion of impulse-controlled industrial manipulators," in *Proc. of the seventh Int. Work. on Advanced Motion Control*, 2002, pp. 365–370.
[25] R. Zanasi and R. Morselli, "Third order trajectory generator satisfying velocity, acceleration and jerk constraints," in *Proc. of the IEEE Int. Conf. on Contr. Appl.*, Glasgow, UK, Sept. 2002, pp. 1165–1170.
[26] L. Biagiotti and C. Melchiorri, *Trajectory planning for automatic machines and robots*. Heidelberg, Germany: Springer, Berlin, 2008.
[27] R. Zanasi and R. Morselli, "Discrete minimum time tracking problem for a chain of three integrators with bounded input," *Automatica*, vol. 39, no. 9, pp. 1643–1649, 2003.
[28] O. Gerelli and C. Guarino Lo Bianco, "A discrete-time filter for the online generation of trajectories with bounded velocity, acceleration, and jerk," in *IEEE Int. Conf. on Rob. and Autom., ICRA2010*, Anchorage, AK, May 2010, pp. 3989–3994.
[29] C. Guarino Lo Bianco and O. Gerelli, "Online trajectory scaling for manipulators subject to high-order kinematic and dynamic constraints," *IEEE Trans. on Rob.*, vol. 27, no. 6, pp. 1144–1152, Dec. 2011.
[30] W. Kim, D. Shin, and C. C. Chung, "Microstepping using a disturbance observer and a variable structure controller for permanent-magnet stepper motors," *IEEE Trans. on Ind. Electr.*, vol. 60, no. 7, pp. 2689–2699, 2013.
[31] J. Hu, Z. Wang, H. Gao, and L. K. Stergioulas, "Robust sliding mode control for discrete stochastic systems with mixed time delays, randomly occurring uncertainties, and randomly occurring nonlinearities," *IEEE Trans. on Ind. Electr.*, vol. 59, no. 7, pp. 3008–3015, 2012.
[32] Y.-W. Liang, L.-W. Ting, and L.-G. Lin, "Study of Reliable Control Via an Integral-Type Sliding Mode Control Scheme," *IEEE Trans. on Ind. Electr.*, vol. 59, no. 8, pp. 3062–3068, 2012.
[33] M. V. Basin and P. C. Rodriguez-Ramirez, "Sliding Mode Controller Design for Stochastic Polynomial Systems With Unmeasured States," *IEEE Trans. on Ind. Electr.*, vol. 61, no. 1, pp. 387–396, 2014.
[34] ——, *Sliding Modes in Control and Optimization*. New York, NY: Springer-Verlag, 1992.
[35] R. Morselli, "Nonlinear trajectory generators for motion control systems," Ph.D. dissertation, 2003.
[36] C. Guarino Lo Bianco and F. Wahl, "A novel second order filter for the real-time trajectory scaling," in *IEEE Int. Conf. on Rob. and Autom., ICRA 2011*, Shanghai, China, May 2011, pp. 5813–5818.
[37] R. Bucher and S. Balemi, "Rapid Controller Prototyping with Matlab/Simulink and Linux," in *6th IFAC Symp. on Adv. in Control Educ., ACE2003*, Oulu, Finland, Jun. 2003.

Corrado Guarino Lo Bianco graduated with honors in Electronic Engineering and received the Ph.D. degree in Control System Engineering from the University of Bologna, Italy, in 1989 and 1994, respectively. Currently, he is with the Dipartimento di Ingegneria dell'Informazione of the University of Parma as Aggregate Professor on Industrial Robotics. He is involved in researches concerning mobile and industrial robotics and, in particular, in the following topics: smooth and optimal trajectory planning, kinematics, dynamics, and control.

Fabio Ghilardelli acquired, with honors, the Bachelor and the Master Degrees in Computer Engineering from the University of Parma, Italy, in 2008 and 2011, respectively. Currently, he is with the Dipartimento di Ingegneria dell'Informazione of the University of Parma as Ph.D Student. He is involved in researches concerning the analysis and the control of robotic manipulators.